AIP | Applied Physics Letters

Spin injection properties in trilayer graphene lateral spin valves

Y. P. Liu, H. Idzuchi, Y. Fukuma, O. Rousseau, Y. Otani et al.

Citation: Appl. Phys. Lett. **102**, 033105 (2013); doi: 10.1063/1.4776699
View online: http://dx.doi.org/10.1063/1.4776699
View Table of Contents: http://apl.aip.org/resource/1/APPLAB/v102/i3
Published by the American Institute of Physics.

Spin injection properties in trilayer graphene lateral spin valves

Y. P. Liu,[1,2] H. Idzuchi,[2,3] Y. Fukuma,[2,4] O. Rousseau,[2] Y. Otani,[2,3,a)] and W. S. Lew[1,a)]
[1]*School of Physics and Mathematical Sciences, Nanyang Technological University, 21 Nanyang Link, Singapore 637371*
[2]*Advanced Science Institute, RIKEN, 2-1 Hirosawa, Wako 351-0198, Japan*
[3]*Institute for Solid State Physics, University of Tokyo, Kashiwa 277-8581, Japan*
[4]*Frontier Research Academy for Young Researchers, Kyushu Institute of Technology, 680-4 Kawazu, Iizuka 820-8502, Japan*

(Received 11 October 2012; accepted 2 January 2013; published online 23 January 2013)

We report on the electrical injection and detection of spin accumulation in trilayer-graphene/MgO/Permalloy lateral spin-valve (LSV) structure. Non-local spin valve signal is clearly observed in the LSV, indicating that spin coherence extends underneath all ferromagnetic contacts. We also show that low-resistivity graphene/MgO/Py junctions enable efficient spin injection and detection in LSV with high applied current density, which leads to large spin accumulation of 120 μV at room temperature. A spin diffusion length of 1.5 μm was obtained for the injector-detector separation dependence of spin valve signal measurements carried out at room temperature, while at T = 10 K, the diffusion length increases to 2.3 μm. © *2013 American Institute of Physics*. [http://dx.doi.org/10.1063/1.4776699]

Graphene has attracted considerable interest in spintronics recently because of weak spin-orbit interaction and also weak hyperfine interaction,[1–3] giving rise to the possibility that graphene can be explored as a spin injection medium with long spin lifetimes even at room temperature. However, the spin relaxation time deduced from the experimental measurements in the graphene lateral spin-valve (LSV) structure are much shorter (0.05−1.2 ns)[4–10] compared to the theoretical prediction (100 ns to 1 μs).[3] The spin relaxation mechanism has been investigated theoretically and experimentally, but this is still under debate. The extrinsic mechanism of the spin relaxation such as charge impurities from the substrate and ripples of the graphene is pointed out theoretically.[3,11,12] However, the spin relaxation time of the high-quality suspended graphene is about 150 ps.[13]

The spin transport properties of few-layer graphene have been recently investigated because impurity potential of the surface is screened by outer layers.[8–10] Han and Kawakami[10] reported that the dominant spin transport mechanism in bilayer graphene is of the Dyakonov-Perel type, whereas that in monolayer graphene is dominated by the Elliot-Yafet mechanism.[10] Trilayer graphene has a unique band structure, where its energy-momentum relationship is composed of both linear (monolayer) and parabolic parts (bilayer).[14,15] Owing to the complex band structure, the charge transport properties in trilayer graphene have been found to be different from that in monolayer and bilayer graphene materials.[16] The spin transport and relaxation properties may be modified by its complex band structure.[17,18] However, the spin transport properties in trilayer graphene are still not yet fully established, partly due to the challenging device fabrication process. In this letter, we demonstrate electrical injection and detection of the spin accumulation in trilayer-graphene /MgO/Permalloy (Py) LSVs. The MgO interface layer functions as a barrier to increase the spin dependent interface resistance, and to reduce the conductivity mismatch issue.[19] A clear spin valve signal ΔR_S of 150 mΩ for low bias current of 0.05 mA is observed at room temperature for LSV with the injector-detector separation of 1.2 μm. The detected voltage change ΔV_S increases with increasing the applied current and then reaches to 120 μV for 1 mA. The dependence of the nonlocal spin valve signal on the injector-detector separation has been investigated and a fitted result has produced a spin diffusion length of 1.5 μm at room temperature and of 2.3 μm at T = 10 K.

A standard non-local geometry with four contacts was used to measure the spin signal of the lateral spin valve structure, as schematically shown in Fig. 1(a). The trilayer graphene samples were prepared using mechanical exfoliation techniques. The number of graphene layers was confirmed by micro-Raman spectroscopy following the 2D-band deconvolution procedure.[20–24] Figure 1(b) shows the characteristic Raman spectra, where the G peak and 2D band features are clearly distinguishable. The number of graphene layers can be identified from the full-width half maximum of the 2D band. Patterned contact lines were fabricated on Si/SiO_2/graphene using conventional photolithography techniques. The contact lines, which consist of bilayer Ti (5 nm)/Au (30 nm) structure, were deposited using electron beam evaporation technique at a base pressure of 1×10^{-7} Torr. To suppress inhomogeneous spin accumulation underneath the detector in LSVs, the trilayer graphene with 2 μm width was defined by the photolithography and oxygen plasma etching. Spin injector and detector electrodes were patterned on the graphene with MMA/PMMA bilayer resist by electron beam lithography. After the developing process, the surface of the graphene was cleaned using ultraviolet radiation technique. A 1.0-nm-thick MgO layer was first grown onto the resist-patterned graphene sample using electron beam evaporation technique and subsequently a 40 nm thick Py layer is grown. Finally, the Py electrodes are capped with a 5 nm thick MgO layer for protection. Figure 1(c) shows an optical micrograph of the fabricated LSV, in which a dark contrast strip lying across the patterned electrodes is the trilayer graphene wire. The widths of the fabricated Py contacts

a)Authors to whom correspondence should be addressed. Electronic addresses: yotani@issp.u-tokyo.ac.jp and wensiang@ntu.edu.sg.

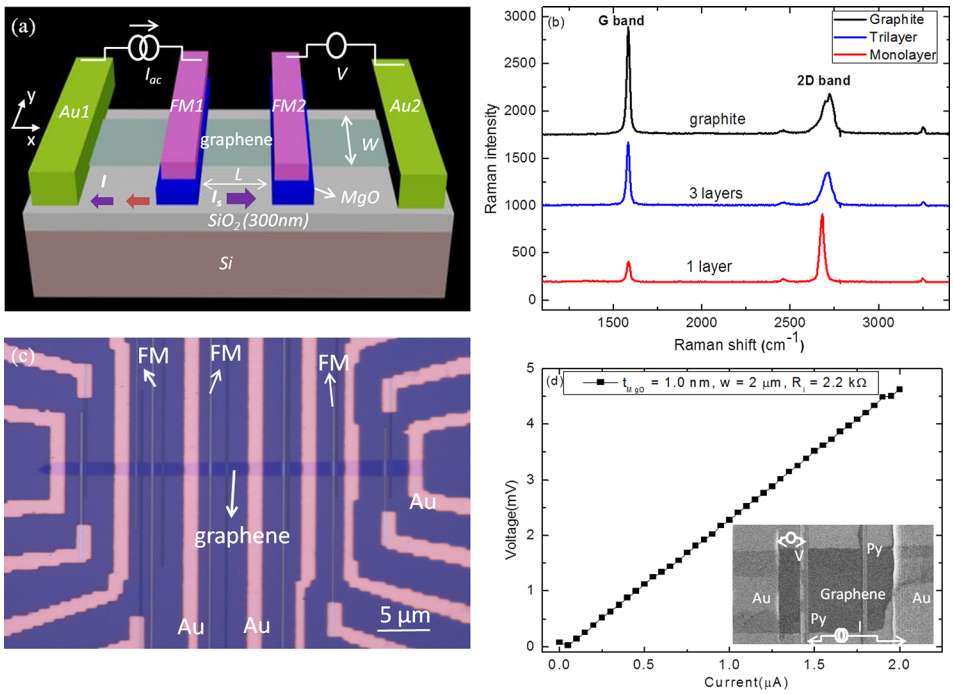

FIG. 1. (a) Schematic drawing of non-local measurement configuration of the trilayer-graphene/MgO/Py lateral spin-valve structure. Spin polarized current I is injected along the arrow on the left-hand side in trilayer graphene. Pure spin current I_S diffuses in the other side of the graphene and then the spin accumulation is detected at the detector. Magnetic field was applied along the easy axis of the Py electrodes during the measurement. (b) Raman spectra of monolayer, trilayer graphene, and graphite. The position of G peak and the spectral features of 2D band confirm the number of atomic layer of the graphene. (c) Optical image of the measurement spin-valve device with electrical contacts for each Py electrode. (d) Room temperature current-voltage (I-V) measurement. The measured interfacial resistance is 2.2 kΩ. Inset shows the schematic picture of the measurement configuration and a scanning electron microscope (SEM) image of LSV fabricated in this study.

were varied from 70 nm to 300 nm so that a variation of coercivity can be obtained. To measure the interfacial resistance of the graphene/MgO/Py junctions, a cross junction configuration was applied, as illustrated in the inset of Fig. 1(d). Figure 1(d) shows the measured current-voltage (I-V) characteristic at room temperature. From this characteristic, the interfacial resistance value of the graphene/MgO/Py junction is measured at 2.2 kΩ (corresponding to 1.2 kΩ μm^2), with a good reproducibility. The graphene/MgO/Py junction showed lower interface resistance than that for typical tunnel junction[13] and a linear I-V characteristic. In our previous studies for metallic LSVs with Py/MgO/Ag junctions,[25–28] the amount of oxygen was found to be decreased in the MgO layer. Such oxygen vacancies decrease the barrier height of the tunneling and the interface resistance.[29]

The non-local spin injection measurements were carried out by applying a magnetic field parallel to the Py wires. A standard lock-in technique with an applied ac current I of 79 Hz and 0.05-1.00 mA was used. Spin-polarized electron is injected into the graphene from the Py injector through the MgO interface layer. Upon injection, spins accumulate at the interface and diffuse in the graphene wire. The spin diffusion is typically described by spin-dependent chemical potentials ($\mu_\uparrow$ and $\mu_\downarrow$), where the spin density in the graphene with a splitting of the chemical potential and the density of spins decays exponentially as a function of the spin diffusion length.[30] Detection voltage V depends on magnetic configuration of Py electrodes and its difference is detected as

$$\Delta R_S = \frac{V_P - V_{AP}}{I} = \frac{\Delta V_S}{I}, \tag{1}$$

where V_P and V_{AP} are, respectively, the voltage with parallel and anti-parallel configurations. Figure 2(a) shows the spin signal V/I as a function of the applied field for a typical LSV configuration with a pair of injector and detector with the separation L of 1.2 μm. The high and low signals correspond to the parallel and antiparallel configuration of the two Py wires. Spin valve signal ΔR_S is clearly observed without tilt of nonlocal resistance as the voltage change, implying no

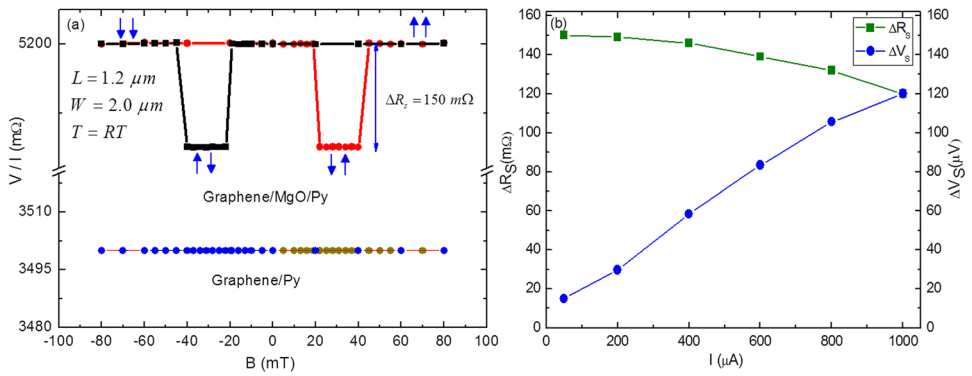

FIG. 2. Room temperature non-local spin valve measurements of the trilayer graphene lateral spin-valve structures. (a) Typical non-local magnetoresistance with two Py electrodes configuration with and without MgO insulator barrier. The measured non-local magnetoresistance change from parallel to antiparallel configuration is $\Delta R_S = 150$ mΩ, which is due to spin injection and transport across the $L = 1.2$ μm gap between the FM1 and FM2 electrodes. (b) Non-local spin-valve signal and voltage as a function of applied bias current at the injector at $T = 300$ K. The injector-detector separation is 1.2 μm and the thickness of the MgO layer is 1.0 nm.

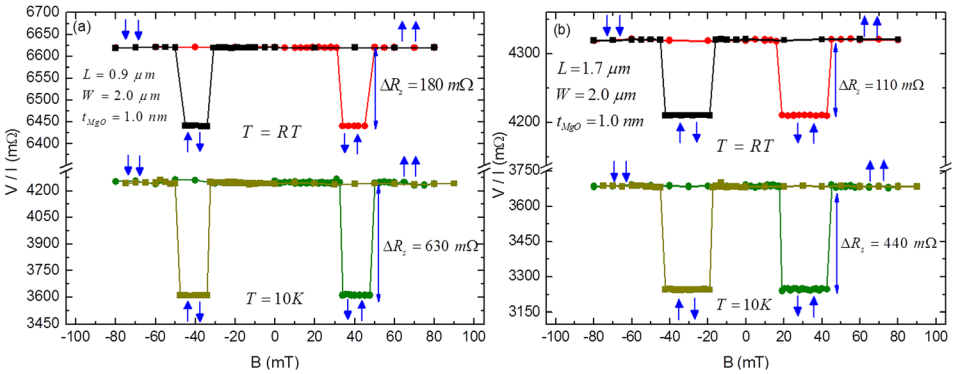

FIG. 3. Separation and temperature dependence of non-local magnetoresistance measurements in trilayer graphene. The measurements show that the ΔR_S value decreases from 180 mΩ (a) to 110 mΩ (b) as the injector-detector separation increases from 0.9 μm to 1.7 μm at room temperature. At $T = 10$ K, the ΔR_{NL} value is relatively larger and when the separation increases, there is also a decrease of the ΔR_S value from 630 mΩ (a) to 440 mΩ (b).

spurious effects such as anisotropic magnetoresistance. The magnitude of 150 mΩ with the injected current 50 μA is observed at room temperature. Figure 2(b) shows the bias current dependence of ΔR_S and $\Delta V_S = \Delta R_S I$. The ΔV_S value increases as the strength of the bias current is increased, however, ΔR_S decreases at high bias current. The spin injection efficiency for such a low resistive junction does not depend strongly on the bias current.[25,27] The decrease of ΔR_S in high bias currents is attributed to Joule heating because the maximum current of 1 mA in Fig. 2(b) gives a current density of 2×10^9 A/m^2 at the junction and 5×10^{11} A/m^2 in the trilayer graphene wire. Note that even with such a large current density the non-local measurement demonstrates spin injection, transport and detection in the LSVs, and a large spin accumulation of 120 μV is realized at room temperature.

In order to study the spin transport property of the trilayer graphene wire, the L dependence of ΔR_S has been investigated. Figures 3(a) and 3(b) show the measured spin signal for LSVs with L of 0.9 μm and 1.7 μm at room temperature, respectively. The results show that ΔR_S decreases from 180 mΩ to 110 mΩ as L increases from 0.9 μm to 1.7 μm because of the spin relaxation in trilayer graphene. Similar measurements were also carried out at low temperature, as shown in Figs. 3(a) and 3(b). At $T = 10$ K, ΔR_S decreases from 630 mΩ to 440 mΩ as L increases 0.9 μm and 1.7 μm. The analytical expression of ΔR_S, for the case whereby the interface resistance is enough higher than the spin resistance of the non-magnetic wires R_N, is approximated by a solution of the one-dimensional (1D) spin diffusion equation[31]

$$\Delta R_S = P_I^2 R_N e^{-L/\lambda_N} \ (R_i \gg R_N), \tag{2}$$

where P_I is the interfacial polarization, R_i is the interface resistance, and λ_N is the spin diffusion length. The obtained experimental data for the L dependence of ΔR_S are well fitted by Eq. (2) with adjustable parameters of P_I and λ_N, as shown in Fig. 4. The fitted P_I and λ_N values are 0.038 and 1.5 μm at room temperature, and 0.065 and 2.3 μm at 10 K, respectively. Note that the 1D spin diffusion model has an excellent agreement with the experimental results. The spin diffusion length obtained in this study is similar to that reported for mono and few-layer graphene on a Si/SiO_2 substrate.[11,13] In order to overcome the spin resistance mismatch between Py and the trilayer graphene, interfacial resistance of the graphene/MgO/Py junction over $R_N = R_G \lambda_N / w_N \sim 2$ kΩ is necessary, where R_G is the measured resistance and w_N is the width of the non-magnetic wire.[8] Thus, the interface resistance of 2 kΩ for the trilayer-graphene/MgO/Py in this study can reduce the spin resistance mismatch problem, which yields spin injection efficiency I_S/I of about 4% and 7% at 300 K and 10 K, respectively. This allows us to evaluate the density of spin current in the graphene as $I_S = P_I \times I/2 = 2 \times 10^{10}$ A/m^2. The observed I_S of the order of 10^{10} A/m^2 suggests that trilayer graphene be useful platform for the application of spin dynamics induced by spin current in LSVs, with the long spin diffusion length even at room temperature.[32–35]

In conclusion, non-local spin valve measurements with trilayer-graphene/MgO/Py lateral spin-valve structures showed that an MgO layer can reduce the conductivity mismatch issue. The maximum spin valve signal ΔR_S of 630 mΩ for low bias current of 0.05 mA is observed for LSV with the separation of 0.9 μm. The detected voltage change ΔV_S increases with increasing applied current and the spin accumulation reaches to 120 μV for 1 mA. Spin diffusion analysis shows that ΔR_S as a injector-detector separation reasonably decreases as the length increases and the spin diffusion length in trilayer graphene is 1.5 μm at room temperature and 2.3 μm at T = 10 K. The high spin accumulation and the long spin diffusion length at room temperature suggest that

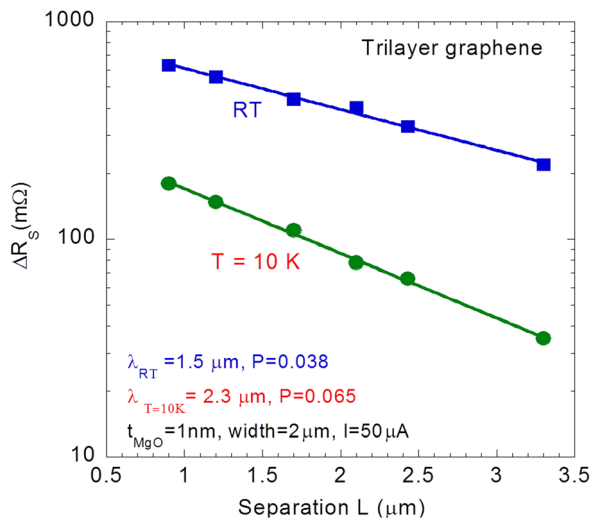

FIG. 4. Spin diffusion characteristics of trilayer-graphene: injector-detector separation (L) dependence of the ΔR_S. Fittings in 1D spin diffusion equation give a spin diffusion length of 1.5 μm and 2.3 μm at room temperature and $T = 10$ K, respectively.

trilayer grapheme offers a promising playground to study spin dynamics by using spin current and the application of devices such as the magnetic field sensor.

This work was supported by the NRF-CRP program (Multifunctional Spintronic Materials and Devices). The authors thank Sun Li and Sugimoto Satoshi for their assistance in experimental measurements, and Dr. Aoki for his helpful discussion.

[1]D. Huertas-Hernando, F. Guinea, and A. Brataas, Phys. Rev. B **74**, 155426 (2006).
[2]H. Min, J. E. Hill, N. A. Sinitsyn, B. R. Sahu, L. Kleinman, and A. H. MacDonald, Phys. Rev. B **74**, 165310 (2006).
[3]D. Huertas-Hernando, F. Guinea, and A. Brataas, Phys. Rev. Lett. **103**, 146801 (2009).
[4]N. Tombros, C. Jozsa, M. Popinciuc, H. T. Jonkman, and B. J. van Wees, Nature **448**, 571 (2007).
[5]M. Ohishi, M. Shiraishi, P. Nouchi, T. Nozaki, T. Shinjo, and Y. Suzuki, Jpn. J. Appl. Phys., Part 2 **46**, L605 (2007).
[6]N. Tombros, S. Tanabe, A. Veligura, C. Jozsa, M. Popinciuc, H. T. Jonkman, and B. J. van Wees, Phys. Rev. Lett. **101**, 046601 (2008).
[7]W. Han, K. Pi, W. Bao, K. M. McCreary, Y. Li, W. H. Wang, C. N. Lau, and R. K. Kawakami, Appl. Phys. Lett. **94**, 222109 (2009).
[8]T. Maassen, F. K. Dejene, M. H. D. Guimaras, C. Jozsa, and B. J. van Wees, Phys. Rev. B **83**, 115410 (2011).
[9]T. Y. Yang, J. Balakrishnan, F. Volmer, A. Avsar, M. Jaiswal, J. Samm, S. R. Ali, A. Pachoud, M. Zeng, M. Popinciuc *et al.*, Phys. Rev. Lett. **107**, 047206 (2011).
[10]W. Han and R. K. Kawakami, Phys. Rev. Lett. **107**, 047207 (2011).
[11]A. H. Castro Neto and F. Guinea, Phys. Rev. Lett. **103**, 026804 (2009).
[12]P. Zhang and M. W. Wu, New J. Phys. **14**, 033015 (2012).
[13]M. H. D. Guimaraes, A. Veligura, P. J. Zomer, T. Maassen, I. J. Vera-Marun, N. Tombros, and B. J. van Wees, Nano Lett. **12**, 3512 (2012).
[14]A. K. Geim and K. S. Novoselov, Nature Mater. **6**, 183 (2007).
[15]A. K. Geim, Science **324**, 1530 (2009).
[16]M. F. Cracium, S. Russo, M. Yamamoto, J. B. Oothinga, A. F. Morpurgo, and S. Tarucha, Nat. Nanotechnol. **4**, 383 (2009).
[17]J. Fabian and S. Das Sarma, J. Vac. Sci. Technol. B **17**, 1708 (1999).
[18]H. Idzuchi, Y. Fukuma, L. Wang, and Y. Otani, IEEE Trans. Magn. **47**, 1545 (2011).
[19]G. Schmidt, D. Ferrand, L. W. Molenkamp, A. T. Filip, and B. J. van Wees, Phys. Rev. B **62**, R4790 (2000).
[20]Y. P. Liu, W. S. Lew, S. Goolaup, H. F. Liew, S. K. Wong, and T. J. Zhou, ACS Nano. **5**(7), 5490 (2011).
[21]L. M. Malard, M. A. Pimenta, G. Dresselhaus, and M. S. Dresselhaus, Phys. Reps. **473**, 51 (2009).
[22]Y. P. Liu, S. Goolaup, C. Murapaka, W. S. Lew, and S. K. Wong, ACS Nano **4**(12), 7087 (2010).
[23]I. Calizo, I. Bejenari, M. Rahman, L. Guanxiong, and A. A. Balandin, J. Appl. Phys. **106**, 043509 (2009).
[24]Y. P. Liu, W. S. Lew, S. Goolaup, Z. X. Shen, L. Sun, T. J. Zhou, and S. K. Wong, Carbon **50**(6), 2273 (2012).
[25]Y. Fukuma, L. Wang, H. Idzuchi, and Y. Otani, Appl. Phys. Lett. **97**, 012507 (2010).
[26]L. Wang, Y. Fukuma, H. Idzuchi, and Y. Otani, J. Appl. Phys. **109**, 07C506 (2011).
[27]Y. Fukuma, L. Wang, H. Idzuchi, S. Takahashi, S. Maekawa, and Y. Otani, Nature Mater. **10**, 527 (2011).
[28]L. Wang, Y. Fukuma, H. Idzuchi, G. Yu, Y. Jiang, and Y. Otani, Appl. Phys. Exp. **4**, 093004 (2011).
[29]W. Wulfhenkel, M. Klaua, D. Ullmann, F. Zavaliche, J. Kirschner, R. Urban, T. Monchesky, and B. Heinrich, Appl. Phys. Lett. **78**, 509 (2001).
[30]P. C. Van Son, H. van Kempen, and P. Wyder, Phys. Rev. Lett. **58**, 2271 (1987).
[31]S. Takahashi and S. Maekawa, Phys. Rev. B **67**, 052409 (2003).
[32]B. Dlubak, M. B. Martin, C. Deranlot, B. Servet, S. Xavier, R. Mattana, M. Sprinkle, C. Berger, W. A. De Heer, F. Petroff, A. Anane, P. Seneor, and A. Fert, Nat. Phys. **8**, 557 (2012).
[33]T. Yang, T. Kimura, and Y. Otani, Nat. Phys. **4**, 851 (2008).
[34]D. Ilgaz, J. Nievendick, L. Heyne, D. Backes, J. Rhensius, T. A. Moore, M. A. Nino, A. Locatelli, T. O. Mentes, A. von Schmidsfeld *et al.*, Phys. Rev. Lett. **105**, 076601 (2010).
[35]B. Behin-Aein, D. Datta, S. Salahuddin, and S. Datta, Nat. Nanotechnol. **5**, 266 (2010).